



# A fast metal–metal bonded water oxidation catalyst



Sara Goberna-Ferrón<sup>a,1</sup>, Bruno Peña<sup>b,1</sup>, Joaquín Soriano-López<sup>a</sup>, Jorge J. Carbó<sup>c</sup>, Hanhua Zhao<sup>b</sup>, Josep M. Poblet<sup>c,\*</sup>, Kim R. Dunbar<sup>b,\*</sup>, José Ramón Galán-Mascarós<sup>a,d,\*</sup>

<sup>a</sup> Institute of Chemical Research of Catalonia (ICIQ), Av. Paisos Catalans 16, E-43007 Tarragona, Spain

<sup>b</sup> Department of Chemistry, Texas A&M University, College Station, TX 77843, USA

<sup>c</sup> Departament de Química Física i Inorgànica, Universitat Rovira i Virgili, Marcel·lí Domingo s/n, E-43007 Tarragona, Spain

<sup>d</sup> Catalan Institution for Research and Advanced Studies (ICREA), Passeig Lluís Companys, 23, E-08010 Barcelona, Spain

## ARTICLE INFO

### Article history:

Received 5 February 2014

Revised 8 April 2014

Accepted 14 April 2014

Available online 14 May 2014

### Keywords:

Water oxidation

Metal–metal bonded compounds

Ru catalyst

Computational methods

## ABSTRACT

The metal–metal bonded diruthenium (II,II) tetraacetate compound,  $[\text{Ru}_2(\mu\text{-O}_2\text{CCH}_3)_4]$ , is a water oxidation catalyst (WOC) that exhibits oxygen evolution rates as high as  $77 \text{ s}^{-1}$  at ambient conditions, exhibiting comparable catalytic activity over a wide pH range ( $1 < \text{pH} < 10$ ). The turnover conditions of the catalyst remain active for several hours with oxidative deactivation eventually occurring at a slow rate. DFT calculations support a single-site mechanism via water nucleophilic attack, with the most energy demanding process being the very first one electron oxidation step. This is one of the fastest WOCs reported, and the first WOC found in the field of metal–metal bonded chemistry.

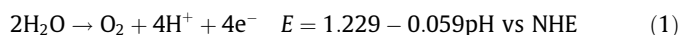
© 2014 Elsevier Inc. All rights reserved.

## 1. Introduction

Dinuclear metal–metal bonded species constitute a large family of transition metal complexes whose flexibility in tolerating a diverse array of ligands allows for exquisite control of their redox and electronic properties [1]. Over the course of many decades, metal–metal bonded molecules and materials with specific structural and physical properties have played prominent roles in diverse fields ranging from catalysis [2–4], crystal engineering [5], magnetism [6–10], spectroscopy [11,12] and anticancer drugs [13–15].

From the perspective of the current work, it is important to note that stable multielectron chemistry of the late transition metal complexes has been exploited for numerous catalytic applications including C–H activation [16], halogen photoelimination [17–19], organometallic transformations [20], photocatalytic hydrogen production [21,22] and oxygen reduction [23,24]. The latter two processes are related to the production of solar fuels which are one of the most attractive alternatives to fossil fuels for environmentally friendly energy solutions. The development of robust and efficient

catalysts for the production of solar fuels is vital if solar technology is to be widely implemented. The lack of a suitable water oxidation Eq. (1) catalyst is one of the main bottlenecks to achieving this goal.



Many transition metal complexes have been reported as homogeneous water oxidation catalysts (WOCs) [25–43], but the state of the art is defined by single-ion or dinuclear Ru complexes supported by N-heterocycles with pyridyl or imidazole groups [44–48]. In light of the importance of Ru(II) chemistry in this field, we rationalized that metal–metal bonded diruthenium complexes could offer some advantages over their mononuclear counterparts if they were found to exhibit activity as WOCs. These species are easily stabilized by available inexpensive ligands such as carboxylates. In addition, the Ru=Ru double bond in the paddlewheel tetracarboxylate compounds based on the  $\text{Ru}_2^{4+}$  core with the electronic configuration  $\sigma^2\pi^4\delta^2\delta^*\pi^2$  increases in strength upon oxidation since antibonding orbitals are being depopulated [1]. With these issues in mind, we set out to explore the catalytic activity of  $[\text{Ru}_2(\mu\text{-O}_2\text{CCH}_3)_4]$  (**Ru<sub>2</sub>**, Fig. 1). Herein, we report the results of water electrolysis experiments that lead to oxygen evolution.

## 2. Experimental

### 2.1. Synthesis

All reagents were commercially available (>99.9%, Sigma–Aldrich) and used without further purification.  $[\text{Ru}_2(\mu\text{-O}_2\text{CCH}_3)_4]$

\* Corresponding authors. Addresses: Departament de Química Física i Inorgànica, Universitat Rovira i Virgili, Marcel·lí Domingo s/n, E-43007 Tarragona, Spain. Fax: +34 977559563 (J. M. Poblet), Department of Chemistry, Texas A&M University, College Station, TX 77843, USA. Fax: +1 9791234567 (K. R. Dunbar), Institute of Chemical Research of Catalonia (ICIQ), Av. Paisos Catalans 16, E-43007 Tarragona, Spain. Fax: +34 977920224 (J.R. Galán-Mascarós).

E-mail addresses: [josepmaria.poblet@urv.cat](mailto:josepmaria.poblet@urv.cat) (J.M. Poblet), [dunbar@mail.chem.tamu.edu](mailto:dunbar@mail.chem.tamu.edu) (K.R. Dunbar), [jrgalan@iciq.es](mailto:jrgalan@iciq.es) (J.R. Galán-Mascarós).

<sup>1</sup> These authors contributed equally to this paper.

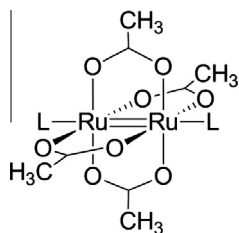


**Fig. 1.** Schematic representation of the molecular structure of  $[\text{Ru}_2(\mu\text{-O}_2\text{CCH}_3)_4]$ . The acetate ligands are bound to the  $\text{Ru}^{2+}$  core in the equatorial positions; L denotes open axial positions for solvent or anion binding.

$(\text{Ru}_2)$  and  $\text{Ru}_2(\mu\text{-O}_2\text{CCH}_3)_4\text{Cl}$  were prepared according to literature methods [1,2].

## 2.2. Electrochemistry

All experiments were performed with a Biologic SP-150 potentiostat. Cyclic voltammetry experiments were performed with a  $0.07\text{-cm}^2$  glassy carbon button working electrode, a Pt wire counter electrode and a Ag/AgCl (NaCl 3 M) reference electrode in 1 M  $\text{NaNO}_3$  milli-Q water, with 50 mM sodium phosphate ( $\text{NaP}_i$ ) buffer. The working electrodes were polished with  $3\ \mu\text{m}$  and  $1\ \mu\text{m}$  diamond paste and rinsed with distilled water prior to use. Cyclic voltammograms were collected in the 0–2.0 V range (vs normal hydrogen electrode, NHE) at different scan rates between 1 and 100 mV/s and different  $\text{Ru}_2$  concentrations between 0.1 and 2 mM.

Bulk water electrolyses were carried out with stirring in a two-chamber cell, with a porous frit connecting both chambers. A Pt mesh counter electrode was placed in one chamber. The other chamber contained a FTO-coated glass working electrode (Pilkington NSG TEC 15A 2.3 mm slides with 12–14  $\Omega/\text{sq}$ . surface resistivity) and a BASi Ag/AgCl (NaCl 3 M) reference electrode. FTO slides were cleaned prior use by sonication for 10 min in alkaline soapy solution (LABWASH), deionized water and isopropanol, followed by annealing at 400 °C for 30 min. Typical electrolysis experiments were carried out in a 50 mM  $\text{NaP}_i$  buffer (pH 7) with 1 M  $\text{NaNO}_3$ . Compensation for ohmic drop was applied by using the positive feedback compensation implemented in the instrument. Oxygen evolution was determined with an Ocean Optics NeoFOX oxygen sensing system equipped with a FOXY probe inserted into the head-space of the anodic compartment.

## 2.3. Electrochemical quartz crystal microbalance

Simultaneous bulk water electrolysis and piezoelectric gravimetry measurements were collected with an SRS QCM-200 microbalance and a Biologic SP-150 potentiostat. Both instruments were computer-controlled with the BioLogic EC-Lab software. A conventional three-electrode cell configuration was used, with a platinum wire as counter electrode, and a BASi Ag/AgCl (NaCl 3 M) as the reference. The working electrode was a 25.4 mm diameter quartz crystal (5 MHz, AT-cut, plano-plano, provided by MicroVacuum Ltd.) coated with a ITO conducting surface (approximate electroactive surface area:  $1.4\ \text{cm}^2$ ). The quartz crystal disk was mounted in the SRS QCM-200 quartz crystal holder. The frequency response of the quartz crystal was monitored before and during experiments. The frequency response was calibrated by electrodeposition of metallic Cu from a 1 mM  $\text{CuCl}_2$  water solution to calculate the equivalence factor in order to transform frequency variations to deposited mass.

## 2.4. Methods

Scanning electron microscopy (SEM) and electron dispersive X-ray spectroscopy (EDX) analysis were performed with a JEOL-JSM6400 microscope equipped with an Oxford EDX analyzer (Oxford Instruments). Mass spectrometry measurements were made using an Omnistar TM GSD 301 C (Pfeiffer) quadrupole mass spectrometer apparatus. All solutions were degassed prior to use. The composition of the gas phase ( $\text{O}_2\ m/z = 32$ ;  $\text{N}_2\ m/z = 28$  and  $\text{CO}_2\ m/z = 44$ ) was measured during controlled potential electrolysis at 1.5 V (vs NHE) using a FTO-coated glass working electrode. A two compartment H-cell separated by a frit was used for these experiments. The working compartment contained the FTO-coated glass working electrode, the Ag/AgCl (NaCl 3 M) reference electrode and the MS-spectrometer cannula and was filled with 20 mL of a  $\text{Ru}_2$  (0.5 or 1 mM) solution in 50 mM  $\text{NaP}_i$  buffer with 1 M  $\text{NaNO}_3$  as the electrolyte. The second compartment of the electrochemical cell contained the platinum mesh auxiliary electrode and was filled with 20 mL of buffer. The solutions were capped with a septum and stirred vigorously.

## 2.5. Computational methods

Calculations were performed with the *Gaussian09* program package [49]. All geometries were fully optimized in the gas phase at the M06-L level [50–52] of density functional theory. The Stuttgart ECP28MWB contracted pseudopotential basis set [53] was used on Ru and the 6-31G(d) basis set [54–57] on all other atoms. The nature of all stationary points was verified by analytical computation of vibrational frequencies, which were also used for calculation of free energy contributions. The determination of energetics required single-point calculations in the solvent phase employing the SMD continuum solvation model [58], in order to account the effects associated with water.

## 3. Results and discussion

### 3.1. Electrocatalytic water oxidation

The electrochemical properties of diruthenium tetracarboxylate-bridged species are highly solvent dependent [59]. The presence of coordinating anions or neutral ligands in the axial positions also exerts a strong influence on the redox potentials. In organic solvents,  $\text{Ru}_2$  typically exhibits a single  $\text{Ru}_2^{+5/+4}$  reversible couple in the 0.2–0.5 V range vs NHE [60–62] (all potentials in this work are referenced to NHE). A perusal of the literature revealed that the aqueous electrochemistry of  $\text{Ru}_2$  has not been well investigated, although in one report it was described to be analogous to that observed in organic solvents [63]. We found quite different behavior (Fig. 2, left, a). At pH 1 (dilute sulfuric acid solution), no distinct reversible redox processes were evident in the cyclic voltammograms of  $\text{Ru}_2$  (0.5 mM) but a feature indicative of a catalytic water oxidation wave above 1.40 V was present. When the sweep was extended to cathodic potentials, a broad irreversible peak was observed below  $-0.3\ \text{V}$  (Fig. 2, left) which corresponds to the irreversible  $\text{O}_2/\text{O}_2^-$  reduction [64]. The feature appears only after successive scans, in support of effective catalytic  $\text{O}_2$  evolution.

When the pH was slowly increased by addition of NaOH, a quasi-irreversible redox couple appeared above pH 2 with peak potentials at  $E_{\text{ox}} = 1.24\ \text{V}$  and  $E_{\text{red}} = 1.05\ \text{V}$  ( $E_{\text{ox}} - E_{\text{red}} = 200\ \text{mV}$ ) which is assigned to the  $\text{Ru}_2^{+5/+4}$  couple. The large  $E_{\text{ox}} - E_{\text{red}}$  difference in water suggests that electron transfer could be associated with proton transfer and the change in going from  $\text{H}_2\text{O}$  to  $\text{OH}^-$  in the axial position stabilizes the  $\text{Ru}_2^{+5}$  redox state. The current associated with the

Download English Version:

<https://daneshyari.com/en/article/61082>

Download Persian Version:

<https://daneshyari.com/article/61082>

[Daneshyari.com](https://daneshyari.com)